

The Infrared Nucleus of the Wolf-Rayet Galaxy Henize 2-10¹

S. C. Beck²

School of Physics and Astronomy of the Sackler Faculty of Exact Sciences and Wise
Observatory; Tel Aviv University, 69978 Ramat Aviv, Israel

and

D. M. Kelly^{2,3}, J. H. Lacy

Department of Astronomy/McDonald Observatory, University of Texas, Austin, TX 78712

Received _____; accepted _____

¹Wise Observatory Preprint 96/77

²Guest Observers, Infrared Telescope Facility, which is operated by the University of Hawaii under contract through NASA.

³Currently at Wyoming Infrared Observatory, University of Wyoming, Laramie, WY 82071-3905

ABSTRACT

We have obtained near-infrared images and mid-infrared spectra of the starburst core of the dwarf Wolf-Rayet galaxy He 2-10. We find that the infrared continuum and emission lines are concentrated in a flattened ellipse 3-4'' or 150 pc across which may show where a recent accretion event has triggered intense star formation. The ionizing radiation from this cluster has an effective temperature of 40,000 K, corresponding to $30M_{\odot}$ stars, and the starburst is $0.5 - 1.5 \times 10^7$ years old.

Subject headings: Galaxies: Individual (He 2-10) — Galaxies: Starburst — Infrared: Galaxies

1. Introduction and Observations

He 2-10 is a blue compact dwarf galaxy and the first galaxy in which Wolf-Rayet emission features were seen (Allen, Wright, & Goss 1976). It contains a bright star cluster A and a fainter cluster B 380 pc ($8''$ at the assumed distance of 9.2Mpc) to the east of A. The outer isophotes of the galaxy are smoothly elliptical. The kinematics of the molecular and atomic gas (Kobulnicky et al. 1995) show that He 2-10 is probably the moderately advanced merger of two dwarf galaxies. Optical spectroscopy (Vacca & Conti 1992) found hundreds of WR and thousands of O stars in the brighter cluster A, and HST UV images (Conti & Vacca 1994) show that the hot stars are grouped into knots the size and mass of globular clusters but from 1 to 10 Myr old. He 2-10 is thus a “starburst dwarf”. Starburst dwarfs differ in important ways from other starburst galaxies: they are objects whose non-burst star formation rate is almost nil, they have low metallicity compared with larger galaxies, and their star formation is not driven by the dynamical mechanisms that dominate in spiral galaxies.

We set out to study the current stellar population of the starburst in He 2-10, with the hope of deducing the history of star formation activity in this galaxy and finding what may have caused it. It is known (Kawara, Nishida, & Phillips 1989) that the brightest region of He 2-10 is actually heavily obscured. We therefore observed this galaxy in the infrared where the extinction will be relatively small. We obtained spectra of the important infrared emission lines in the $8 - 13\mu\text{m}$ region with the Irshell spectrograph (described in Lacy et al. 1989) at the NASA IRTF in May 1995. A wavelength region equivalent to 950 km s^{-1} was scanned around each of the [Ne II] $12.8\mu\text{m}$, [Ar III] $8.99\mu\text{m}$, and [S IV] $10.5\mu\text{m}$ lines. The spectral resolution was about 30 km s^{-1} . The slit was $2''$ wide and sampled by 11 pixels along its $11''$ length. It was oriented NS for the [Ne II] measurements and EW for the others. The telescope drifted by as much as $1-2''$ during a ten minute observation. The

weather was good for the [Ne II] and [Ar III] observations but unstable for the [S IV], so we will use a [S IV] measurement with the same instrument from ESO made available to us by J.M. van der Hulst. The infrared line fluxes and details of the observations are in Table I and a typical [Ne II] spectrum is shown in Figure 1. We used a card at ambient temperature and standard stars for flux calibration and the results are accurate to 20%. The data were reduced and analysed with the SNOOPY package (Achtermann 1992).

We also present in Figure 2 J, H and K band continuum images obtained for us as a service observation by Mr. Charles Kaminski using the NSFCAM on the NASA IRTF. The spatial scale on these figures is 0.3'' per pixel, and the FWHM of stars in the field is 0.9''. The images were reduced and analysed with the VISTA package. Each image in figure 2 is the sum of two or three exposures in that band which were flatfielded with dome flats. The exposure times were different in each band and totalled 6 sec at J, 48 sec at H, and 60 sec at K; the galaxy was at least 35000 counts above the sky background even in these short exposures. We have not attempted to flux-calibrate the images.

2. Spatial Extent and Structure of the Starburst

2.1. The Infrared Continuum

Optical observations of He 2-10 show that continuum and line emission are strongly concentrated in a small clump (Vacca & Conti's A) in the center of the main body of the galaxy. Corbin, Korista, & Vacca's (1993) images show that the central source in the inner 10'' extends towards PA 127 (in degrees east of north) in $H\alpha$ and in the V band. The V-band image of the entire galaxy has a halo at PA 168, which Corbin et al. believe is the major axis of the object. At 10 μ m Sauvage, Lagage, & Thuan (1995) found an HII region NW of the main clump which they identify with the $H\alpha$ extension in that direction. The

near-infrared images in J,H, and K bands are less affected by extinction than is the optical and have the further advantage that they are good bands for locating giant and supergiant stars and dust-obscured O and B stars. The J,H, and K images in Figure 2 look very much alike; they each show an elongated ellipse of dimension (defined from the contour which is 10% of peak above the background) about 5x3 arcsec extended in PA 130, which we will hereafter call "the disk" (because it looks like a disk, not because there is any data on its rotation). If the brightest point of the disk is the center of the galaxy then the disk is not symmetric around the center but extends further to the NW than to the SE, and on the NW side of the center has a slightly less acute (to NS) angle. We believe that both these effects are due to unresolved subsources, notably the $10\mu\text{m}$ H II region, probably the small clusters of hot stars seen in the UV images, but possibly others which are still unknown, rather than to a bar structure. The logs of the ratios of J/K, J/H and K/H, which are equivalent modulo a constant to the relative J-K, J-H and K-H colors, are in Figure 3. There are no obvious structures that could be attributed to dust lanes. (It should be noted that the infrared aperture photometry of Johansson (1987) is on a much larger scale; the entire disk lies inside the smallest aperture used there.)

We see that all the tracers of active star formation are concentrated in the NIR disk. In addition to the near and middle infrared emission and the $H\alpha$ described above, the UV star clusters found by Conti & Vacca (1994) appear to lie across the disk in a bent line (bent in the same sense as the shift across the center seen in the NIR). We suggest that the UV star clusters lie on the near, less-heavily obscured side of the disk.

How does the NIR disk, the locus of current star formation, relate to the overall structure of the galaxy and its merger history? The accreted CO has a velocity structure reminiscent of a galaxy disk with the maximum velocity gradient in PA 130, agreeing with the NIR disk. The brightest CO is at PA 150, much closer to the PA 160 angle of the

galactic halo (Kobulnicky et al. 1995). We suggest that the NIR disk is the original disk of the galaxy and that accreted CO falling onto it is fueling the burst of star formation seen in the UV and IR. That the galactic halo is at a different angle than the disk may record an offset between disk and halo that predates the accretion event. It is also possible that the accretion process itself, which is well-advanced and probably at least 10^8 years old, distorted the angle of the galactic halo. This form of merger has been little studied so this suggestion must remain tentative.

It should be noted that the 3.6 cm radio continuum observations of Kobulnicky (1996), the CO observations of Kobulnicky et al. (1995), and the H_2 measurements of Baas, Israel, & Koorneef (1994) do not agree with the infrared continuum and emission lines. The peak of CO emission is $2''$ ENE of A, as is a strong source of 3.6 cm radio emission, and the peak of shocked H_2 is offset 1-3'' east from A. It is probable that the CO marks a body of gas not currently forming stars and that the H_2 is shock excited by winds from the starburst impacting the molecular cloud. It is harder to explain the offset between the 3.6 cm radio continuum and the starburst. That region of the galaxy may be so blanketed by extinction that even the 2 and 10 μm continua and 12.8 μm [Ne II] emission cannot penetrate; this would be consistent with the concentration of molecular gas in that area. Or, the 3.6 cm emission may be from supernovae and trace an older stage of the starburst which does not currently have detectable infrared continuum or line emission, in which case it should be strong at 20cm (although measurements at 20cm with the spatial resolution needed to separate the 3.6 cm emission peak from A will be hard to achieve).

2.2. The [Ne II] Lines

We attempted to derive the size of the [Ne II] emission line source by comparing the Irshell data on [Ne II], the strongest line observed, to stellar profiles. The PSF for the run

in which these data were obtained was somewhat elliptical due to an optical misalignment, which limits the accuracy of this method, but we can say that the [Ne II] emission on peak A is 3'' in diameter in both dimensions (with a probable error of 0.5''). The spatial resolution of the [Ne II] is enough lower than the infrared and UV images that the disk structure seen in the infrared and the small star clusters seen in the UV could not be distinguished even if present. We will therefore refer to the emission source detected in [Ne II] as the star cluster. This will provide consistency with the accepted use of cluster A and B for the bright optical sources. But we think it possible and even likely that it will break up into smaller and more structured sources under higher resolution.

The secondary 10 μ m H II region was not mapped in [Ne II]. We looked for [Ne II] on B and did not detect it, which is consistent with the relative strengths of the two clusters in other wavelengths and is further argument that star formation in cluster B, while it exists, is at too low a level to be called a starburst.

If the kinematics of the [Ne II] are like those of the CO and HI, the FWHM would be 50-80 km s⁻¹. Our lines were broadened by a misalignment of the dewar optics, but they showed similar profiles to the [Ne II] observed on the same night in the Galactic H II region W33. The lines in W33 are expected to be no more than 50 km s⁻¹ wide, so we place an upper limit on the lines in He 2-10 of FWHM \leq 100 km s⁻¹.

The common practise of quoting “the” extinction to a galaxy is misleading: galaxies and the dust within them can have complex three-dimensional structures. It is somewhat more precise to discuss the extinction to a given component of a galaxy. Vacca & Conti’s (1992) optical spectroscopy of He 2-10 found $E_{(B-V)} = 0.56$ or $A_v = 1.7$ mag to region A. Such a high value for A_v implies that the optical observations could not see through the source. The infrared Brackett line measurements of Kawara et al. (1989), which will probe deeper into the source, found A_v of about 17 mag, which is consistent with the depth of

the $10\mu\text{m}$ silicate feature and the molecular column observed by Kobulnicky et al. (1995). He 2-10 is therefore like NGC 5253 (Beck et al. 1996) and many other galaxies where optical and UV observations see the near side of the star forming region and longer wavelength measurements see deeper in. The extinction in the infrared, while lower than in the optical, is not negligible. Unfortunately the mid-infrared extinction law is not well known and seems to differ in different environments (Draine 1989); furthermore, the dependence of extinction on the metallicity is unknown. Extinction laws in the literature give results ranging from 0.6 mag at [Ne II] and about 1.7 mag at [Ar III] and [S IV] (Becklin et al. 1978) to 0.22 mag at [Ne II] and 0.55 mag at [Ar III] (Roche & Aitken 1984) for $A_v = 17$ mag. We will discuss the importance of this uncertainty below.

3. Stellar Population and Star Burst History

3.1. Stellar Population

The O star population of the obscured region can be found from the mid-infrared and Brackett lines. First, we compared the ratios of the [Ne II], [Ar III] and [S IV] line fluxes to the model H II region grid of Sutherland, Shull, & Beck (1996) to find the effective temperature of the exciting stars. We use models with $z = 0.1z_\odot$, the closest in the grid to the almost $0.2z_\odot$ oxygen value of He 2-10 (Conti & Vacca 1994), and assume that Ne:Ar:S is solar. The models have $\log(n_e) = 4.0$, which is typical of dense starburst regions, and $\log U$ (the ionization parameter) -2.5 and -1.5.

The [Ne II]/[Ar III] ratio is a good stellar temperature diagnostic for temperatures less than 45,000 K as it is fairly insensitive to density, ionization parameter and filling factor. The [Ar III] and [Ne II] were not observed in identical locations nor at the same slit angles, so we have compared the total flux in the EW slit position on region A where [Ar III] was

observed to the total [Ne II] flux observed in each of the NS [Ne II] slit positions. This assumes that the distribution of the infrared lines is spherically symmetric, which within the resolution of the observations it appears to be; the uncertainties introduced by possible small asymmetries will be less than those from other factors such as extinction. The results uncorrected for reddening between 12.8 and 8.99 μm give stellar temperatures of 36-38,000 K for the different [Ne II] slit positions. Any extinction correction will increase [Ar III] relative to [Ne II] and give hotter temperatures; both the Becklin et al. (1978) and the Roche & Aitken (1984) extinction curves give stellar temperatures 38-40,000 K. These results are very insensitive to the metallicity and will be the same within the uncertainties for solar metal content. The weakness of [Ne II]/[Ar III] ratio is that it is relatively insensitive to small temperature shifts in precisely the 36,000 K to 41,000 K range where He 2-10 falls. The [Ne II]/[S IV] ratio (comparing the total observed [Ne II] flux to the total observed [S IV] flux) gives stellar temperatures above 37,000 K, but this ratio, although it has a large dynamic range, is very sensitive to the ionization parameter and the metallicity. If we compare the ratios of [Ar III], [S IV], and [Ne II] to those seen in the Galactic Center and NGC 3256 where the effective stellar temperature has been derived from the much more sensitive [Ne II]/[Ne III] ratio (Kunze et al. 1996) and interpolate, we find a temperature of $39,000 \pm 1400$ K, consistent with what the [Ne II]/[Ar III] ratio gives.

The stellar temperatures (38,000-40,000 K) found from the infrared lines are equivalent to O6.5 ZAMS stars (Panagia 1973). The ionizing spectrum of a cluster of stars will differ from that of a single star, so it is only an approximation to treat the cluster as if it were composed only of one stellar type. While we expect there to be many stars cooler than 40,000 K the weak [Ar III] and [S IV] rule out the presence of more than a very few stars hotter than 40,000. Cluster simulations (Kunze et al. 1996) show that the upper mass cutoff in a cluster is typically about $5M_{\odot}$ greater than the single-star equivalent mass, so the upper mass cutoff is about $35M_{\odot}$. We can use Ho, Beck, & Turner’s (1990) result

which relates the total luminosity of a star cluster to the ionization (with a slight correction because we use a different upper mass cutoff) and find that the total stellar luminosity needed for the Lyman continuum flux $N_{Ly\alpha}$ of 7.6×10^{52} to $1.1 \times 10^{53} \text{ s}^{-1}$ (found from the extinction corrected $Br\alpha$ flux) is $3.7 - 5.3 \times 10^9 L_{\odot}$. This is quite close to the $8 \times 10^9 L_{\odot}$ of total luminosity from the IRAS FIR flux of He 2-10. The FIR beam of course contains the whole galaxy while the Brackett lines are limited to the core; He 2-10 is another example of the common starburst galaxy phenomenon that the bulk of the infrared luminosity observed by IRAS with large beams is generated by massive stars in a very small area (Ho et al. 1990).

The stellar luminosity derived from the infrared lines may be compared to that observed at optical and ultraviolet wavelengths. The cluster observed in the infrared is about a factor of 10 more luminous than the 5500 O stars that Vacca & Conti (1992) find from optical spectra. The ultraviolet observations of Conti & Vacca (1994) find about 6 times as many O stars as their optical measurements; this may be due, as Conti & Vacca suggest, to a combination of larger area coverage and contributions from evolved stars, but the dependance of their result on the very large extinction correction at 220nm may also be a factor; a small change in the proper extrapolation from E_{B-V} to A_{220} can change the final luminosity by more than a factor of two. In any case, the luminosity of the star cluster derived from the infrared lines is at least twice as great and may be 5-10 times as great as the optical luminosity. This is the expected result when the extinction is so great that the optical measurements do not see through the source.

The total mass of the obscured star cluster can be calculated from the observed ionization if we assume a mass function. If we take a mass function that goes as $M^{-3.2}$, assume that stars smaller than 10_{\odot} do not contribute significantly to the ionization and sum the ionization of stars from 35 to $10 M_{\odot}$ using Panagia's (1973) results for the ionizing

flux of a ZAMS star of a given temperature and spectral type, we find the total mass of stars between $10M_{\odot}$ and $35M_{\odot}$ is $4.7 - 6.9 \times 10^6 M_{\odot}$ (where the spread in mass reflects the range of total ionization found from the Brackett lines). Giant and supergiant stars produce more ionization at a given spectral type; taking the extreme case that all the stars are luminosity class III reduces the total mass by about a factor of 2. The ZAMS case implies a mass density of $8M_{\odot}pc^{-3}$ in a 130 pc radius, although since the young stars are probably clumped into small clusters like the ones seen in the UV (this may be confirmed when higher spatial resolution infrared observations become possible) this average density is only a lower limit. Kobulnicky et al. (1995) find a dynamical mass of 3.2×10^6 to $4.8 \times 10^7 M_{\odot}$ in the inner 70 pc, but caution that those are only lower limits due to beam size effects. But even within the large uncertainties of both the CO and the infrared measurements, it is clear that a substantial fraction of the dynamical mass in the center is in the form of young massive stars.

3.2. Starburst History

The effective stellar temperature of the cluster, as derived from the mid-infrared lines above, can be used in combination with a set of cluster evolution models to estimate the age and nature of the starburst. The other important constraint on the starburst age is the non-thermal radio flux, which we find by subtracting the 5 GHz thermal flux of $9 - 11mJy$ (derived from the Brackett lines, the range reflects uncertainty in the extinction and the electron temperature) from the total $55mJy$ observed by Allen et al. (1976). (While the radio fluxes were observed with much larger beams than the infrared, we will assume that the radio emission is dominated by the young star cluster and not by extended emission; this is usually the case in star-forming dwarfs.) We follow Allen et al. that the non-thermal radio emission is due to supernovae remnants rather than to the more extreme mechanisms

which occur in radio galaxies; this agrees with the spectral index, the size and structure of the radio emission in the 3.6 cm maps, and the nature of the host galaxy. Then the non-thermal flux shows that a large number, which cannot be calculated exactly because of the wide range of supernova radio brightnesses but which we estimate at a few thousand, of supernovae have exploded in He 2-10. (We believe that the objection of Allen et al. that a large number of supernovae is not consistent with the low metal content of the galaxy may not be valid; He 2-10 has a relatively high abundance of oxygen for a dwarf, 50% higher than NGC 5253 for example, and the amount of O produced in the required number of supernova is consistent with the observed. It would be highly desirable to observe the [O/Fe] ratio in He 2-10 to constrain the contribution of supernovae to the metal content.)

The observations combined with the cluster evolution models of Sutherland et al. (1996) show that the cluster in He 2-10 is unlikely to have formed coevally. A coeval star cluster cools off so fast that its effective temperature will be as high as the observed only at ages less than 2×10^6 yrs, which is not enough time for the SNe needed for the non-thermal radio emission. We turn to gaussian burst models, where the total mass of stars formed is a gaussian function of time, with its peak at 5×10^6 yrs from the start of the burst and a FWHM in time of 4×10^6 yrs, and the chances of a star of a given mass forming at a given time are found from Monte Carlo simulations. (Other scenarios for long-lived star bursts, such as exponentially decaying rates, are of course possible; the gaussian models are at present the best studied.) The effective stellar temperature found from the infrared lines does not constrain the burst age tightly; the cluster age can be from 5×10^6 to 1×10^7 years since the start of the burst in the absence of WR stars and as old as 1.5×10^7 yrs if WR stars are important in the infrared cluster. It similarly does not rule out longer-lived bursts. (It is at present very difficult to detect WR stars in the infrared and there is only a very high upper limit on the possible number of WR stars in the infrared cluster (Lumsden, Puxley, & Doherty 1994), nor can we assume that the stellar population in the obscured

region is like that in the optically visible region.) If we assume that we do not see stars more massive than about $30M_{\odot}$ because they have become supernovae, the cluster must be at least 5×10^6 yrs old (Woosley, Langer & Weaver 1993). The optical and infrared colors indicate that the cluster is about 2×10^7 years old (Johansson 1987); this is somewhat older than our results for the infrared cluster but considering how ill-constrained the age of the infrared cluster is the discrepancy may not be significant. We should remember that only in very unusual cases can a star formation episode be given a unique age; the above numbers probably reflect a star formation rate generally high but fluctuating with time over the last $1 - 2 \times 10^7$ yrs. The optical cluster, for example, contains many WR stars much younger than the cluster age derived from the colors.

3.3. Conclusion

We have found that the infrared emission of He 2-10 is produced by a star cluster 130×180 pc in size, with its ionizing radiation dominated by O6.5 stars, and less than 1.5×10^7 years old. He 2-10 resembles NGC 5253, the most famous bright infrared WR galaxy, in that they are both dominated by condensed central clusters of young OB stars of similar (to within a factor of two) sizes. It appears however to have had a very different history. The star cluster in NGC 5253 probably formed in a coeval burst; star formation in He 2-10 appears to have been a more sustained process. The galaxies are also at different evolutionary stages; the star cluster in He 2-10 may be almost 10 times as old as that in NGC 5253. The young star cluster in He 2-10 has a disk shape and lies at the same angle as the steepest velocity gradient of the recently accreted molecular gas, which is different from the orientations of the galactic halo and the bulk of the CO. We believe that the recent burst of star formation we have observed lies in the original galactic disk and was triggered by the infall of molecular gas from the accretion event. The offset between the disk and the

halo may be the result of the merger process or may have predated the merger.

We thank Mr. Charles Kaminski for obtaining the infrared images and the NASA IRTF for the time, Dr. J.M. van der Hulst for the use of the [S IV] data, and Mr. H.A. Kobulnicky for access to unpublished data and for interesting discussions. This work was supported by the US-Israel Binational Science Foundation grant 94-00303 and by USAF contract F19628-93-K-0011. D.K. is supported at Wyoming by NSF grant AST94-53354.

REFERENCES

- Achtermann, J.M., in ADASS p 451, A.S.P.Conference 25, 1992.
- Allen, D.A., Wright, A.E., & Goss, W.M. 1976, MNRAS, 177, 91
- Baas, F., Israel, F.P., & Koorneef, J. 1994, A&A, 284, 403
- Beck, S.C., Turner, J.T., Ho, P.T.P., Lacy, J.H., & Kelly, D.M. 1996, ApJ, 457, 610
- Becklin, E.E., Matthews, K., Neugebauer, G., & Willner, S.P. 1978, ApJ, 220, 831
- Conti, P.S. & Vacca, W.D. 1994, ApJ, 423, L97
- Corbin, M.R., Korista, K.T., & Vacca, W.D. 1993, AJ, 105, 1313
- Draine, B.L., in Infrared Spectroscopy in Astronomy p 93, ESA SP-290, 1989.
- Ho, P.T.P., Beck, S.C., & Turner, J.T. 1990, ApJ, 349, 57
- Johansson, L. 1987, A&A, 182, 179
- Kawara, K., Nishida, M., & Phillips, M.M. 1989, ApJ, 337, 230
- Kobulnicky, H.A., Dickey, J.M., Sargent, A.I., Hogg, D.E., & Conti, P.S. 1995, AJ, 110, 116
- Kobulnicky, H.A. 1996, private communication
- Kunze, D. et al, 1996, in press at A&A.
- Lacy, J.H., Achtermann, J.M., Bruce, D.E., Lester, D.F., Arens, J.F., Peck, M.C., & Gaalema, S.D. 1989, PASP, 101, 1166
- Lumsden, S.L., Puxley, P.J., & Doherty, R.M. 1994, MNRAS, 268, 82
- Panagia, N. 1973, AJ, 78, 929
- Roche, P.F. & Aitken, D.K. 1984, MNRAS, 215, 269
- Sauvage, M., Lagage, P.O., & Thuan, T.X. 1995. Exp. Astr., 3, 165
- Schaller, P.G., Schaerer, D., Meybet, G., & Maeder, A. 1993, A&AS, 96, 269

Sutherland, R.S., Shull, M. & Beck, S.C. 1996, in prep.

Vacca, W.D. & Conti, P.S. 1992, ApJ, 401, 543

Woosley, S.E., Langer, N., & Weaver, T.A. 1993, ApJ, 448, 315

Fig. 1.— The spectrum of [Ne II] observed with a $2'' \times 11''$ NS slit across the center of peak A.

Fig. 2.— J, H, and K band images of He 2-10 obtained with NSFCAM on the IRTF. a) J band: the first contour is at 16000 counts and the interval is 2500 counts. b) H band: the first contour is at 53000 and the interval is 2000. c) K band: the first contour is at 55000 and the interval is 3000.

Fig. 3.— The logarithms of the a)J/H, b)J/K, and c)K/H map ratios. These are equivalent to the relative J-H, J-K and K-H colors up to a constant.

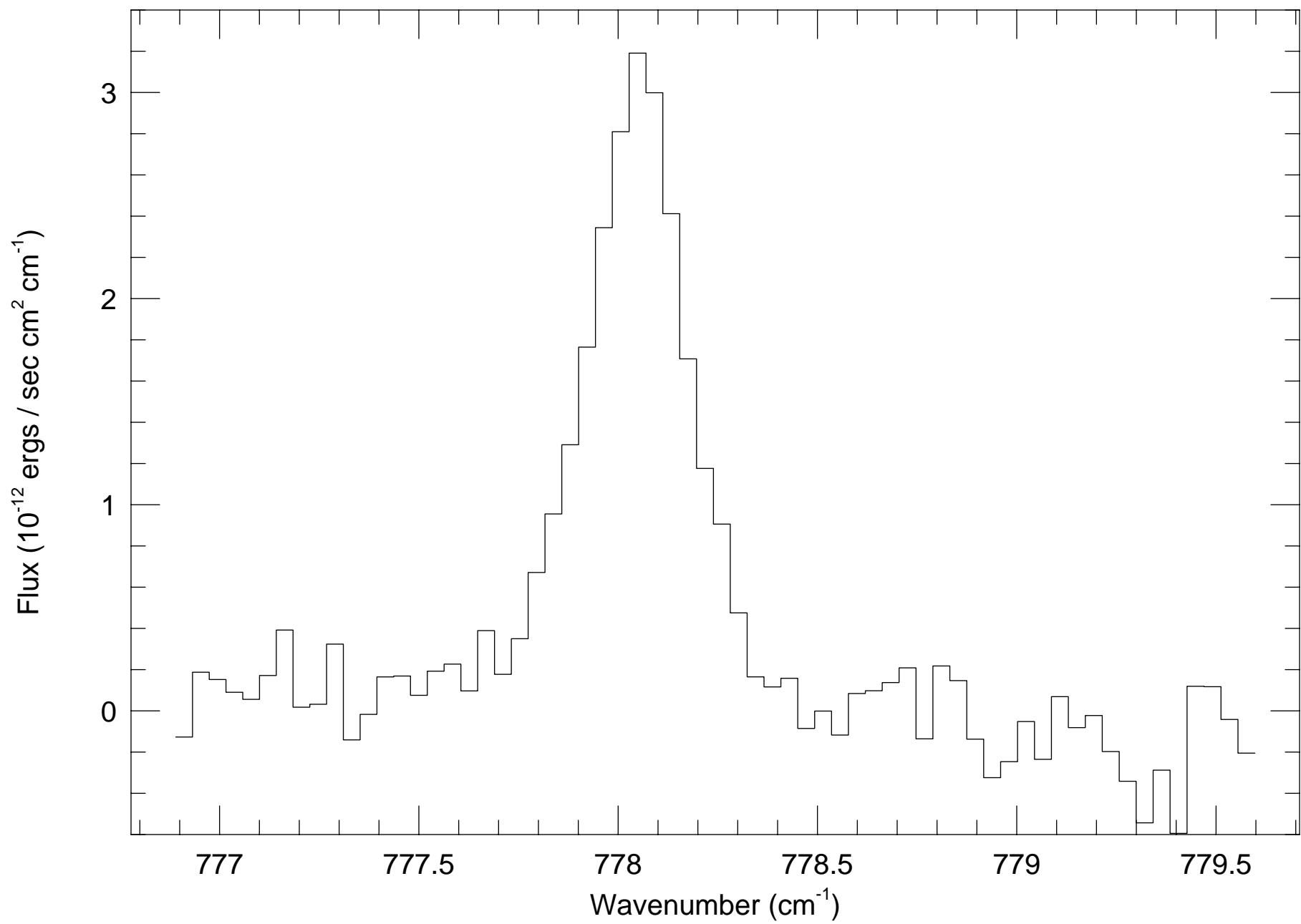


TABLE 1. Observed Line Fluxes

| Species | Wavelength | Date, Site | Slit | Flux($erg\ s^{-1}\ cm^{-2}$) |
|----------|-------------|-----------------|---------|--------------------------------|
| [Ne II] | $12.8\mu m$ | May 1995, IRTF | 2.0" NS | $2 \pm 0.2 \times 10^{-12}$ |
| [Ne II] | $12.8\mu m$ | April 1993, ESO | 1.6" EW | $2.5 \pm 0.5 \times 10^{-12}$ |
| [Ar III] | $8.99\mu m$ | May 1995, IRTF | 2.0" EW | $1.6 \pm 0.5 \times 10^{-13}$ |
| [S IV] | $10.5\mu m$ | April 1993, ESO | 1.6" EW | $5 \pm 3 \times 10^{-14}$ |

Fig. 2a

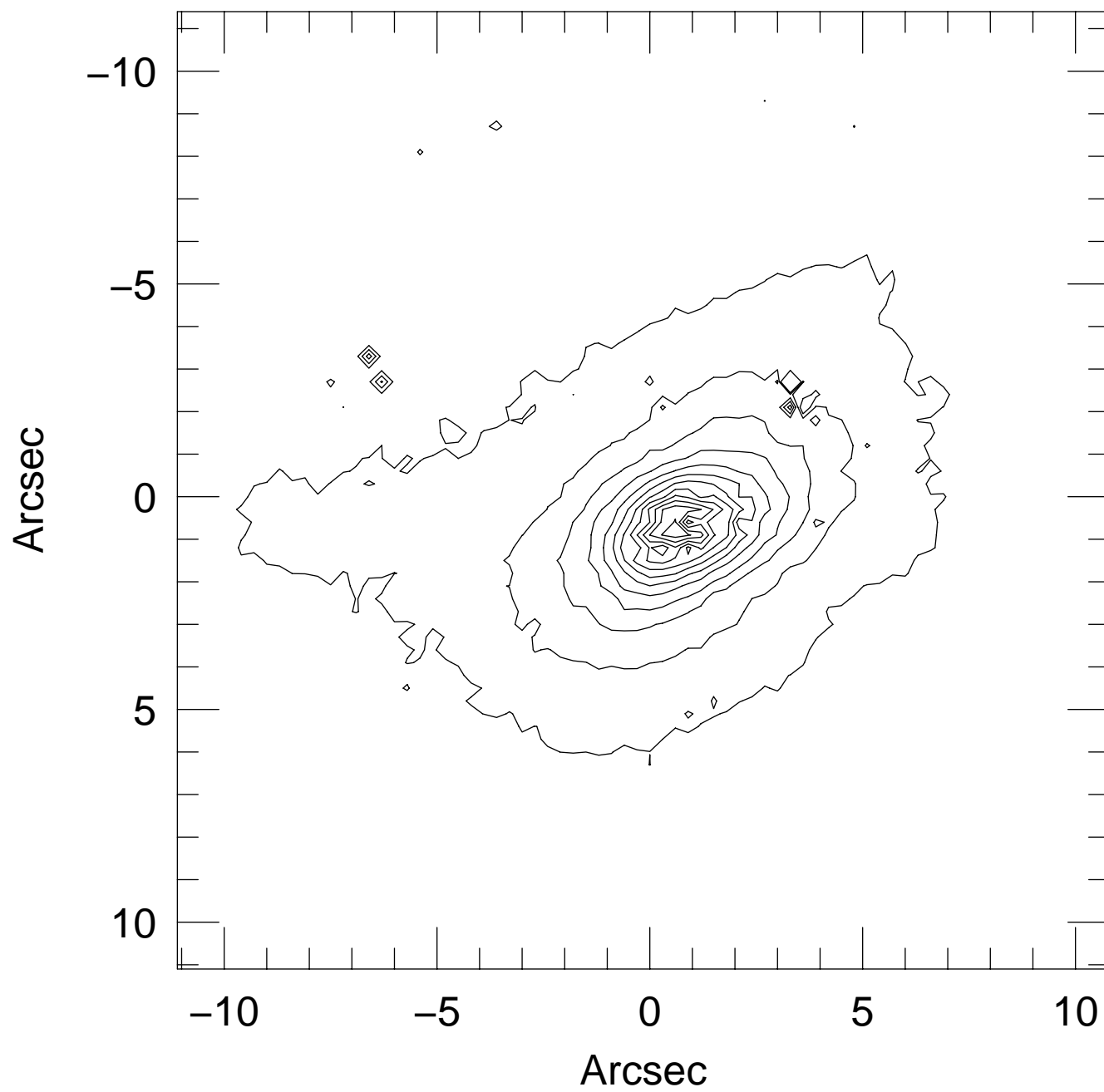


Fig. 2b

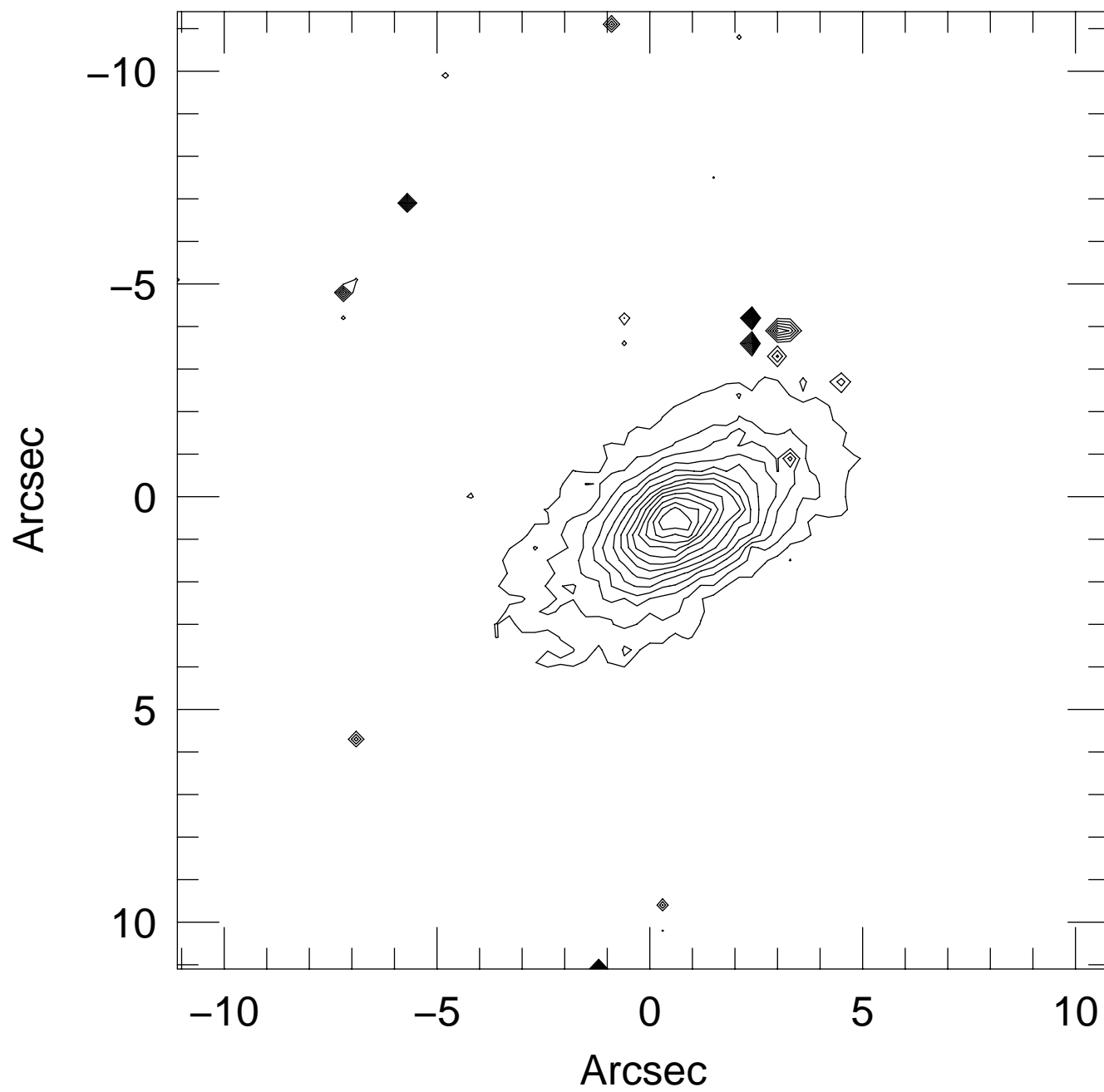


Fig. 2c

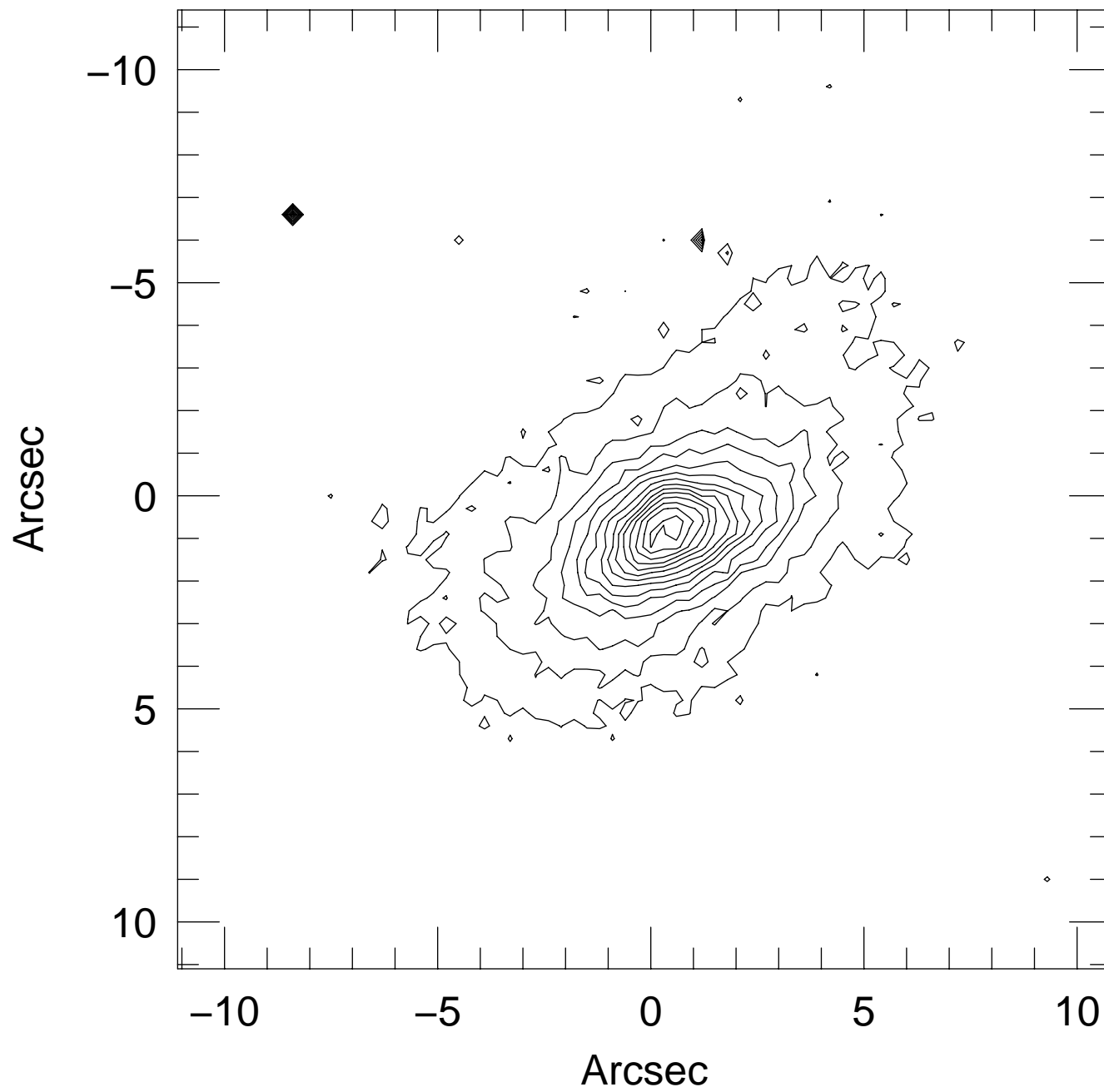


Fig. 3a

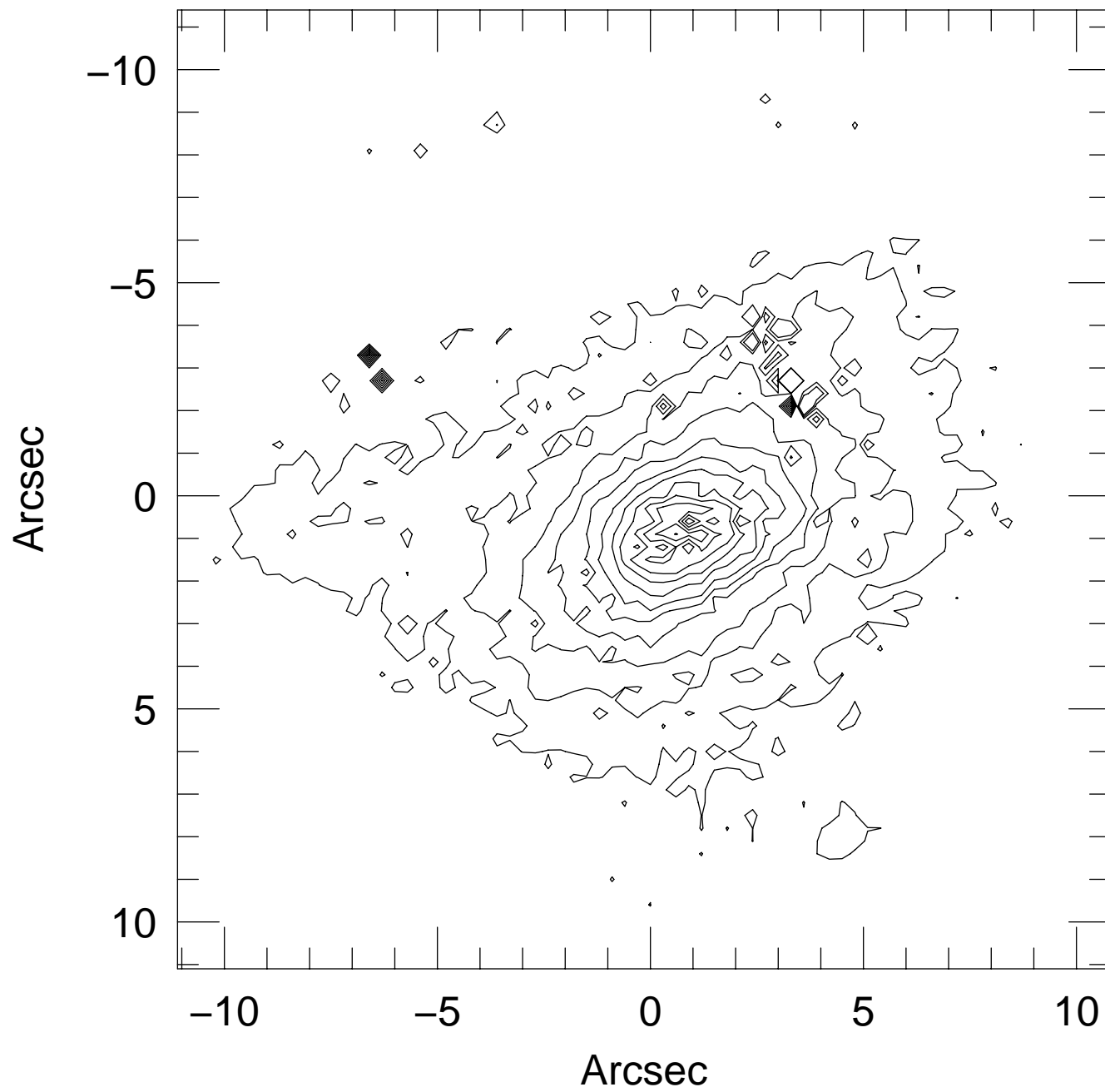


Fig. 3b

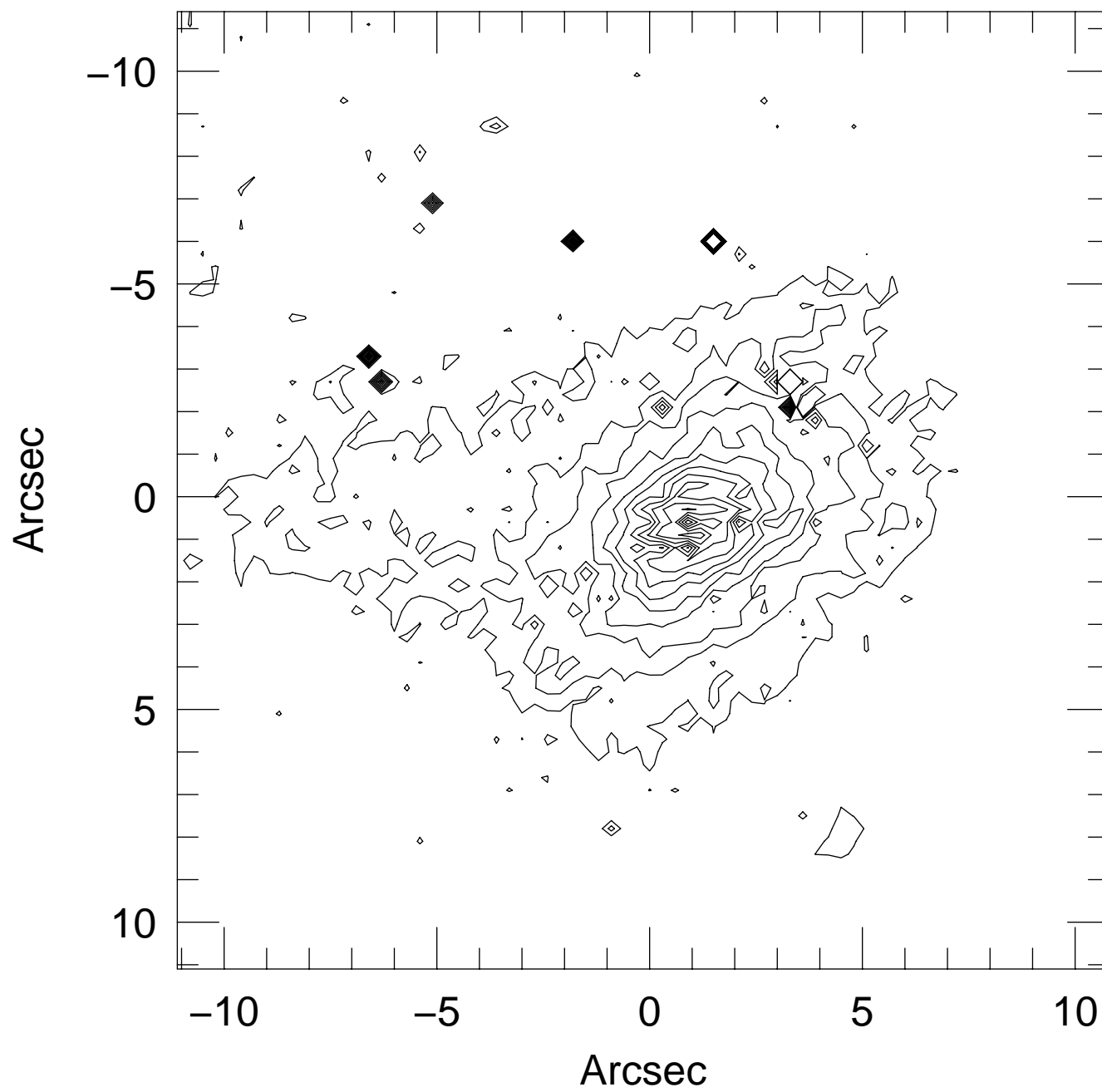


Fig. 3c

